Unmanned Systems, Vol. 10, No. 4 (2022) 343–353

DOI: 10.1142/S2301385022410023

UNMANNED SYSTEMS
https://www.worldscientific.com/worldscinet/us

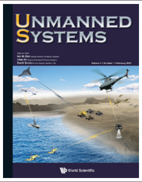

An Immersion and Invariance Controller for Aerial Manipulation

Aarón López Luna[*,‡], Hugo Rodríguez Cortés[‡], Israel Cruz Vega[*], Jose Martinez-Carranza[*,§]

[*]*Instituto Nacional de Astrofísica, Óptica y Electrónica, Puebla, Mexico*

[†]*Centro de Investigación y de Estudios Avanzados del Instituto Politécnico Nacional, Mexico*

For aerial manipulators, a steady flight must be guaranteed to perform safe interaction with the surrounding environment. This paper focuses on the development of a position control algorithm for an aerial manipulator system (AMS). The position control algorithm is based on the Immersion and Invariance (I&I) theory. The proposed controller maintains the position of the aerial manipulator at the desired point under external and internal disturbances. The control architecture uses a Visual-SLAM technique using on-board sensors for AMS positioning. A series of outdoor experimental tests are performed to demonstrate the effectiveness of the proposed control strategy.

Keywords: Immersion and invariance control; aerial manipulation; nonlinear control; UAV system.

1. Introduction

The number of applications in which aerial robots are used has proliferated over recent years. Aerial manipulators are designed to perform physical interactions with the surrounding environment. Aerial manipulation research focuses on improving mechanical designs and control strategies to increase the capability to manipulate objects, exert force on a surface, and use tools in realistic applications [1]. However, technological challenges still need to be addressed before reliable use of such technology becomes possible. Among these challenges, the capability to carry on a manipulator and handle disturbances during the movement of the manipulator is still a difficult challenge for small-size Unmanned Aerial Vehicles (UAVs) but represents an interesting research topic and is the driving goal of this work.

The quadrotor is considered one of the most efficient UAVs for researchers around the world in the aerial manipulation field [2]. Due to the higher manoeuvring capabilities of the quadrotor in comparison with other UAVs. A small-size quadrotor is capable of loading a light-weight manipulator and maintaining a stable flight with a proper control algorithm [3].

The quadrotor is a nonlinear, open-loop, unstable, and underactuated system and the incorporation of a moving robotic arm to the structure increases the disturbance to the system that cannot be easily eliminated by feedback controllers. In order to tackle such problems and to improve the system's performance, researchers have proposed a set of advanced control methods to guarantee a stable flight during the manipulation task, including impedance control [4–6], Backstepping control [7,8], and Proportional-Integral-Derivative (PID) control [9,10] to name a few.

A methodology to design direct and indirect adaptive controllers for nonlinear systems, called Immersion and Invariance (I&I), was proposed in [11]. The I&I method is a control tool based on two classical theories, which are system Immersion and manifold Invariance [12]. The I&I approach captures the desired behavior of the system to be controlled by introducing a target dynamical system. Then, a suitable stabilizing control law is designed to guarantee that the controlled system asymptotically behaves like the target system [13]. Adaptive controllers based on I&I

Received 24 January 2022; Accepted 16 April 2022; Published 8 June 2022. This paper was recommended for publication in its revised form by co-editor-in-chief, Ben M. Chen.
Email Addresses: [†]*aaron.eleazar@inaoep.mx*, [§]*carranza@inaoep.mx*
[*]Corresponding author.

technique for UAV systems were developed in [14,15] as a control solution to maintain the vehicle stable along the desired trajectory, and in [16] a multi-variable finite-time composite control strategy based on I&I was proposed for a quadrotor under unknown disturbances.

Until now, the I&I control approaches for aerial systems described in the literature consider the problem of the position stability for the UAV, but such works do not include the application of the I&I approach to improving the performance of an aerial manipulation system during the movement of the manipulator or the interaction phase and considering for the aerial manipulator from the perspective of proposing one controller to solve the problem. In this paper, the divide and conquer strategy is followed. Thanks to the engineering advances in quadrotor control, they are available in the market aerial vehicles whose position dynamic response to operator inputs can be modeled by first- or second-order systems. Hence, in this paper, the internal commercial quadrotor controller is updated with an external I&I adaptive control loop to solve the position control of an aerial manipulator.

The rest of this paper is organized as follows. Section 2 describes the development of the aerial manipulator, the Visual SLAM method to operate in outdoor scenarios, and the proposed quadrotor model. In Sec. 3, we present the position control strategy based on the I&I theory to maintain the system in the desired position, the experimental setup, and the experimental validation of the proposed controller. Finally, the conclusions of the results and a description of the future work of this research are presented in Sec. 4.

2. Background

Before beginning with this research work, in this section, we mention a background of the investigation, experiments, and results in the aerial manipulation field we achieved in recent years. At the beginning of the research, we developed an aerial manipulator based on a Commercial small UAV (parrot bebop-2) with a 2-DOF arm to study the behavior of the system with the added weight and the disturbances of the arm. The manipulator was designed and implemented based on the technical capabilities of the selected aerial platform. Then, when a stable flight was achieved through a computational compensation control, we improved the capabilities of the proposed aerial manipulator by implementing an external control-loop based on a Gain-Scheduling (GS) PID control strategy to work with the internal bebop-2 controller and mitigate the disturbances induced by the movement of the 2-DOF arm and the contact with a vertical surface.

Rojas-Perez and Martinez-Carranza presented in [17] an obstacle avoidance system based on the Visual SLAM approach to estimate the position of a bebop-2 taking advantage of the on-board camera, and without any other motion capture system to feedback the position of the vehicle to the controller. We combined this estimation pose technique with our aerial manipulation system to extend its capabilities to outdoor scenarios where the use of caption motion systems to sense the pose of the vehicle is limited. Then, we presented a study of the behavior of the system in interaction with a vertical surface in an outdoor environment. To improve the results of previous works, we consider the implementation of the I&I as an alternative to the GS-PID external control due to the capability to increase the robustness of a nonlinear system against disturbances [11]. In the following section, we present the I&I methodology and the implementation of our aerial manipulation system.

2.1. *Aerial manipulation system*

The quadrotor dynamic model assumes a rigid mechanical cross-shaped structure with a rotor mounted at each tip. To describe the quadrotor motion model, two reference axes are considered, the earth and body axes, see Fig. 7. In mixed, body, and earth coordinates, the following set of differential equations will describe the quadrotor dynamic model [18]:

$$\begin{aligned} \dot{X} &= RV^b, \\ m\dot{V}^b + m\Omega \times V^b &= R^\top F_g^e + F_T^b + F_A^b, \\ \dot{R} &= R\Omega^\wedge, \\ J\dot{\Omega} &= -\Omega^\wedge J\Omega + M_T^b + M_A^b, \end{aligned} \tag{1}$$

where $X = [x \quad y \quad z]^\top$ is the translational position with respect to the earth axes, $V^b = [u \quad v \quad w]^\top$ is the translational velocity expressed in body axes, R is the rotation matrix from body to earth axes, and $\Omega = [p \quad q \quad r]^\top$ is the rotational velocity expressed in body axes. Moreover, $(\cdot)^\wedge$ is a map from $\mathbb{R}^3$ to the Lie algebra $\mathfrak{so}(3)$ defined as [19]

$$\mathfrak{so}(3) = \{\omega_1^\wedge \in \mathbb{R}^{3\times3} | \omega_1 \times \omega_2 = \omega_1^\wedge w_2, \forall w_1, w_2 \in \mathbb{R}^3\}.$$

The external forces acting on the quadrotor mechanical structure are given by

$$F_g^e = \begin{bmatrix} 0 \\ 0 \\ mg \end{bmatrix}, \quad F_T^b = \begin{bmatrix} 0 \\ 0 \\ T_T \end{bmatrix}, \quad F_A^b = \begin{bmatrix} \mathbf{q}_d S_f C_X \\ \mathbf{q}_d S_f C_Y \\ \mathbf{q}_d S_s C_Z \end{bmatrix} \tag{2}$$

while the external moments are

$$M_T^b = \begin{bmatrix} M_x \\ M_y \\ M_z \end{bmatrix}, \quad M_A^b = \begin{bmatrix} \mathbf{q}_d S_f \ell C_{M_X} \\ \mathbf{q}_d S_f \ell C_{M_Y} \\ \mathbf{q}_d S_s \ell C_{M_Z} \end{bmatrix}, \tag{3}$$

where T_T is the total thrust generated by the rotors and M_x, M_y and M_z are the moments around the body axes generated by the rotors

$$\mathbf{q}_d = \frac{1}{2}\rho V^2$$

is the dynamic pressure with ρ the air density and

$$V = \sqrt{u^2 + v^2 + w^2}.$$

Additionally, S_f and ℓ are geometric quadrotor characteristics, C_X, C_Y and C_Z are the aerodynamic force coefficients and C_{M_X}, C_{M_Y} the aerodynamic moments coefficients.

In terms of the Tait–Bryan angles [20]

$$\Phi = \begin{bmatrix} \phi \\ \theta \\ \psi \end{bmatrix}$$

with ϕ, θ and ψ the roll, pitch and yaw angles, respectively, the rotation matrix R reads as[a]

$$R(\Phi) = \begin{bmatrix} c_\psi c_\theta & c_\psi s_\theta s_\phi - s_\psi c_\phi & c_\psi s_\theta c_\phi + s_\psi s_\phi \\ c_\theta s_\psi & s_\psi s_\theta s_\phi + c_\psi c_\phi & s_\psi s_\theta c_\phi - c_\psi s_\phi \\ -s_\theta & c_\theta s_\phi & c_\theta c_\phi \end{bmatrix}.$$

Aerial vehicle's internal autopilots shape the system's response at different levels depending on the available sensors. Hence, if rotational states are measured, the internal autopilot can shape the aerial vehicle's response as a second-order system for the translational dynamics and a first-order system for the remaining rotational dynamics. Hence, if the autopilot commands, robustly and arbitrarily fast, this is

$$\lim_{t\to T} \phi = \phi_d, \quad \lim_{t\to T} \theta = \theta_d, \quad \lim_{t\to T} r = r_d \tag{4}$$

for some bounded T, with ϕ_d, θ_d and r_d the desired references for roll, pitch and yaw angular velocity, respectively, the quadrotor dynamics (1) becomes

$$\begin{aligned} \begin{bmatrix} \dot{x} \\ \dot{y} \\ \dot{z} \end{bmatrix} &= \begin{bmatrix} c_\psi c_{\theta_d} & c_\psi s_{\theta_d} s_{\phi_d} - s_\psi c_{\phi_d} & c_\psi s_{\theta_d} c_{\phi_d} + s_\psi s_{\phi_d} \\ c_{\theta_d} s_\psi & s_\psi s_{\theta_d} s_{\phi_d} + c_\psi c_{\phi_d} & s_\psi s_{\theta_d} c_{\phi_d} - c_\psi s_{\phi_d} \\ -s_{\theta_d} & c_{\theta_d} s_{\phi_d} & c_{\theta_d} c_{\phi_d} \end{bmatrix} \begin{bmatrix} u \\ v \\ w \end{bmatrix}, \\ \begin{bmatrix} \dot{u} \\ \dot{v} \\ \dot{w} \end{bmatrix} &= \begin{bmatrix} v r_d \\ -u r_d \\ 0 \end{bmatrix} + g \begin{bmatrix} -s_{\theta_d} \\ c_{\theta_d} s_{\phi_d} \\ c_{\theta_d} c_{\phi_d} \end{bmatrix} + \frac{T_T}{m} \begin{bmatrix} 0 \\ 0 \\ 1 \end{bmatrix} \\ &\quad + \frac{1}{m} \begin{bmatrix} \mathbf{q}_d S_f C_X \\ \mathbf{q}_d S_f C_Y \\ \mathbf{q}_d S_s C_Z \end{bmatrix}, \\ \dot{\psi} &= r_d. \end{aligned} \tag{5}$$

In the reduced quadrotor model (5) the control inputs are ϕ_d, θ_d, r_d and T_T. If, in addition, the translational velocity V^b is measured, the autopilot can be modified to shape the translational dynamics a set of first-order systems. In this case, the autopilot commands, robustly and arbitrarily fast

$$\lim_{t\to T_0} u = u_d, \quad \lim_{t\to T_0} v = v_d, \quad \lim_{t\to T_0} w = w_d$$

for some bounded $T_0 > T$, with u_d, v_d and w_d the velocity references. Hence, the remaining quadrotor dynamics reads as

$$\begin{aligned} \begin{bmatrix} \dot{x} \\ \dot{y} \end{bmatrix} &= \begin{bmatrix} c_\psi & -s_\psi \\ s_\psi & c_\psi \end{bmatrix} \begin{bmatrix} u_d \\ v_d \end{bmatrix}, \\ \dot{z} &= w_d, \\ \dot{\psi} &= r_d. \end{aligned} \tag{6}$$

This is the case with the aerial vehicle used in this work. Using the information from the Attitude Reference and Hedging System as well as optical flow and SLAM algorithms, the internal controller shapes the aerial vehicle as a first-order dynamics expressed in Eq. (6). Now, by commanding the yaw angle to zero, the quadrotor motion model along the x-axis becomes

$$\dot{x} = u_d + \delta \tag{7}$$

with δ the disturbance from the robotic arm, the wall effect, the interaction with a surface, and the unmodeled dynamics.

2.2. *System behavior*

Experimental tests were performed to justify assuming that the proposed aerial manipulator can be modeled as a first-order system. The input signal in all tests is shown in Fig. 1. The first test considers the bebop-2 without the robotic arm. Then, a second test was performed using the same control input with the robotic arm attached to bebop-2.

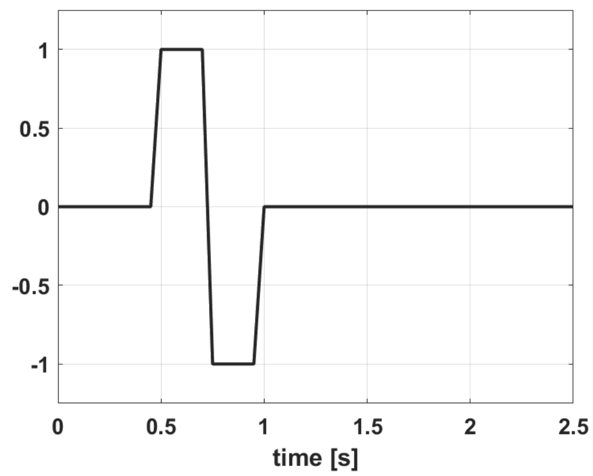

Fig. 1. Test input signal.

[a] In the following, $\cos(x) = c_x$, $\sin(x) = s_x$ for any angle x.

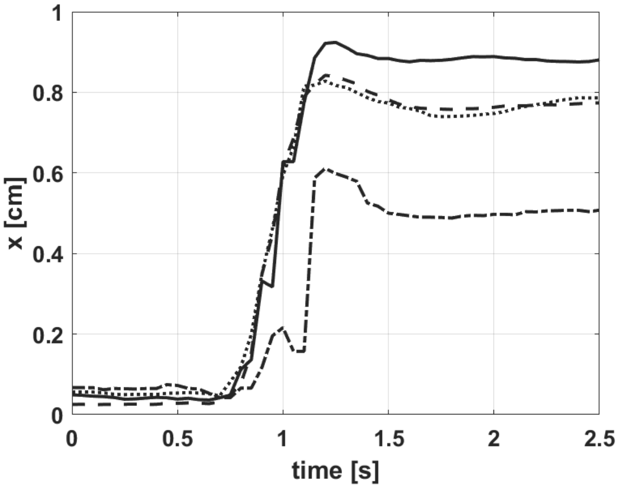

Fig. 2. Bebop-2 response without robotic arm, successful tests. Test 1 (continuous line), test 2 (dashed line), test 3 (dotted line), test 4 (dash-dot line).

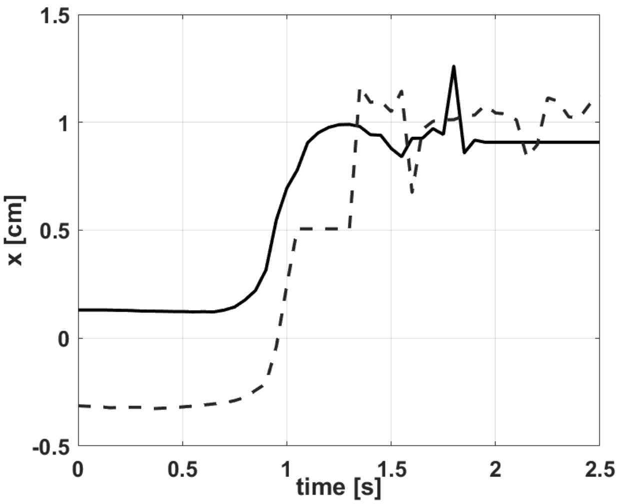

Fig. 3. Bebop-2 response without robotic arm, unsuccessful tests. Test 1 (continuous line), test 2 (dashed line).

Several tests were carried out to obtain meaningful results of the system's response in both experiments. Figure 2 shows the most representative successful results in the first experiment. Figure 3 depicts unsuccessful results due to aggressive movement of the vehicle, which affects the position estimation of the SLAM technique.

The results of the second experiment are shown in Fig. 4 and, as in the first experiment, a set of tests was carried out. Some successful responses of the aerial manipulator are presented in the graphic. Once again, some unsuccessful tests are shown in Fig. 5.

Note that the control input does not have physical units; it only takes the maximum and minimum values accepted by the drone software. Denote by $\mathbf{y}$ the measured position

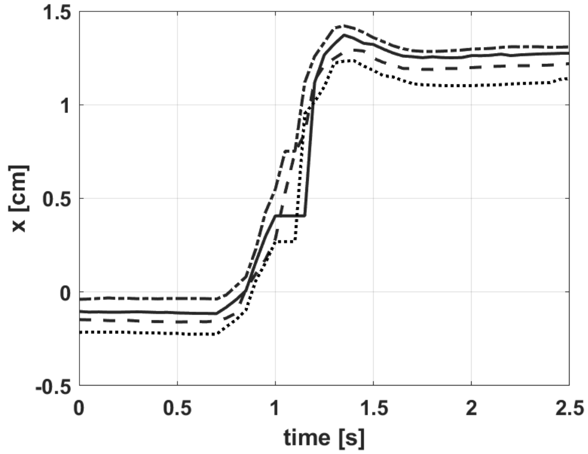

Fig. 4. Bebop-2 response with robotic arm, successful tests. Test 1 (continuous line), test 2 (dashed line), test 3 (dotted line), test 4 (dash-dot line).

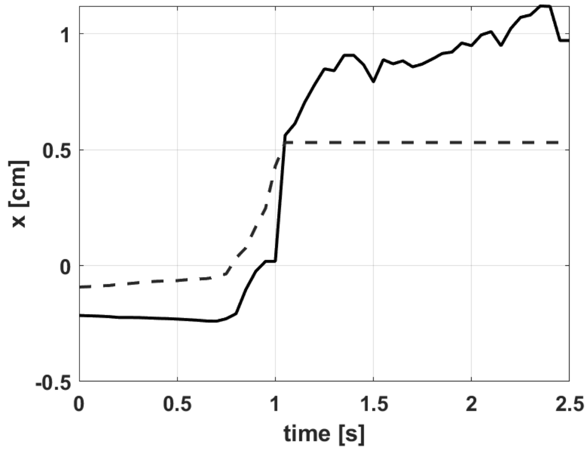

Fig. 5. Bebop-2 response with robotic arm, unsuccessful tests. Test 1 (continuous line), test 2 (dashed line).

response and assume that the drone response can be modeled as follows:

$$\dot{\mathbf{y}} = \theta_1 \mathbf{y} + u \tag{8}$$

with θ_1 a constant parameter. In Eq. (8), the signals $\mathbf{y}$ and u are measurable; moreover $\dot{\mathbf{y}}$ can be computed numerically. Thus, it follows that

$$\mathbf{Y} = \mathbf{y}\theta_1 \tag{9}$$

with $\mathbf{Y} = \mathbf{y} - u$. Using the least squares linear regression method, as reported in [21], the following values are obtained $\theta_1 = 0.3801$ and $\theta_1 = 0.3717$ for tests 1 and 2, respectively. Figure 6 shows the comparison between the drone response and the predicted one for each test.

From the results in Fig. 3, it can be concluded that the proposed model qualitatively captures the Bebop-2 response,

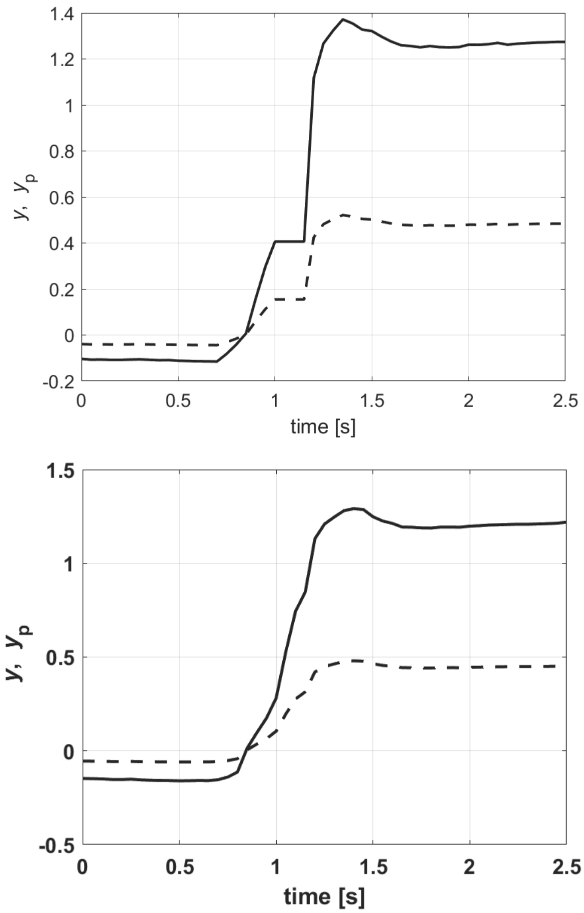

Fig. 6. Test 1. Bebop response (continuous line), predicted response (dashed line). Test 2. Bebop response (continuous line), predicted response (dashed line).

although there is a difference in the response magnitude. Hence, it is assumed that the unmodeled dynamics $\theta_1\mathbf{y}$ and the response magnitude difference are modeled by the disturbance δ so that in the following, it is considered that (7) models the aerial manipulator.

3. Experiments and Results

3.1. *Control algorithm*

Control design in the presence of unknown disturbances is a challenging task. In recent years, two control design approaches have dominated the literature: active disturbance rejection control (ADRC) [22] and sliding mode control, specifically the super twisting algorithm [23]. Both approaches depart from simple mathematical models of the system so that external disturbances and unmodeled dynamics are condensed together in a generic disturbance. Both approaches share the necessity to impose upper bounds on the disturbance. The I&I control method can be adapted to estimate the disturbance and feedback to reject it. The I&I technique also requires assuming that an upper bound on the disturbance is available.

In the I&I technique, the disturbance estimation error is defined as follows:

$$\delta_1 = \delta - \rho_1 - \Gamma x$$

with δ_1 the estimation error, ρ_1 the estimator state, and Γ a positive constant. Thus, if

$$\lim_{t\to\infty} \delta_1 = 0$$

it follows that

$$\lim_{t\to\infty} (\delta - \rho_1 - \Gamma x) = 0$$

so δ is asymptotically reconstructed by $-\rho_1 - \Gamma x$. Straightforward computations show that defining

$$\dot{\rho}_1 = -\Gamma(u_d + \rho_1 + \Gamma x) \tag{10}$$

one gets

$$\dot{\delta}_1 = -\Gamma\delta_1 + \dot{\delta}.$$

Hence, if $\dot{\delta} = 0$, the estimation error δ_1 converges exponentially to zero. Defining the aerial manipulator error as $\tilde{x} = x_d - x$ with x_d the constant desired position, the control input is defined as

$$u_d = k_p\tilde{x} - \rho - \Gamma x. \tag{11}$$

Finally, one gets

$$\begin{aligned} \dot{\tilde{x}} &= -k_p\tilde{x} - \delta_1, \\ \dot{\delta}_1 &= -\Gamma\delta_1, \end{aligned}$$

where the values of gains k_p and Γ are must be selected carefully to obtained the desired behavior. Hence, for any positive gains k_p, Γ, the error signals $\tilde{x} = x_d - x$ and $\tilde{\rho} = \delta - \rho - \Gamma x$ converge to zero.

Thanks to the quadrotor symmetry, the controller for the y position is designed following exactly the same procedure. The control law expressed by Eqs. (11) and (10) is implemented in the aerial manipulator to control the longitudinal and lateral motions of the system to regulate the position in an outdoor scenario and guarantee a stable flight. In the following section, we describe the setup of the experiments to investigate the effectiveness of the proposed control strategy.

3.2. *Experimental setup*

The proposed control strategy was evaluated via experimental tests in an outdoor environment. To reduce the disturbances (mostly due to the environment), an I&I controller was implemented and added to the system.

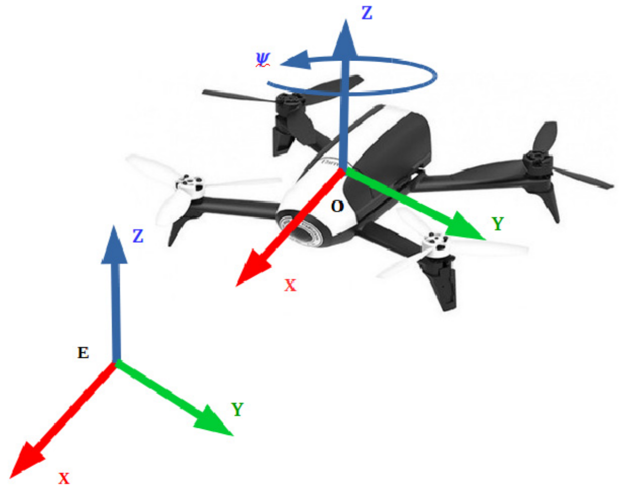

Fig. 7. Aerial system scheme.

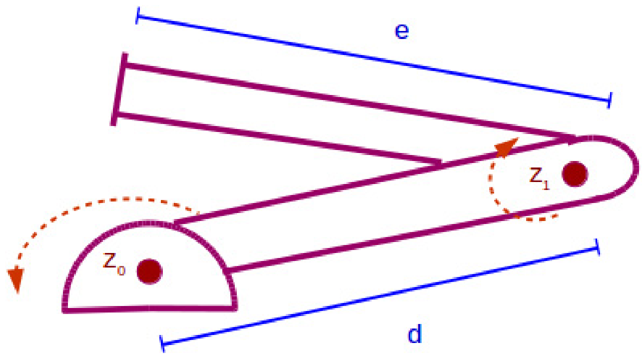

Fig. 8. Manipulator attached to aerial system.

Fig. 9. Outdoor scenario. A carpet is set in the ground to provide more texture for the SLAM technique and improve the pose estimation.

In previous works, we used the VICON camera system to measure the position of the vehicle and feedback the information to the controller [3,24] but, in outdoor environments, the implementation of VICON is laborious and limited. For that reason, in our most recent works, we incorporated the Visual SLAM technique to replace the VICON system in the control structure and to improve the capabilities of our proposed system [25]. The pose estimation using visual SLAM was exploited in [17,26]. The method takes advantage of two characteristics of the aerial vehicle; the on-board camera and the altitude measurement. Due to the features of the aerial platform, we can include the Visual SLAM technique as a pose estimation method in the complete system. The control algorithm runs in a ground station (computer), and we take advantage of the wifi and Bluetooth connection to communicate the computer with the robotic arm and the bebop-2. The coordinate frame of the aerial manipulator is represented by Fig. 7. The longitudinal and lateral motions of the system are represented by the X- and Y-axes. The I&I controller was implemented for both axes; a standard PID controller was also incorporated to control the ψ and Z-axis and guarantee the correct orientation and distance to the ground. To see a video of the experiments performed in this work, see the following URL: https://youtu.be/l_a4L8RlafE.

The robotic manipulator was designed with two degrees of freedom. Each joint produces a rotary movement in axis z_0 and z_1, respectively (see Fig. 8). The length of both links (d,e) is 15 cm; when the robotic manipulator is deployed, it provides a safe distance between a vertical surface and the aerial system. The total weight of the manipulator is 227 g, so the aerial system is capable of flying even with the manipulator attached.

The outdoor scenario can be shown in Fig. 9. In this research work, we decided to put the robotic arm on the top of the vehicle; this allows the sensors below bebop-2 to operate without any kind of obstruction and guarantee a good measurement. This change in the position of the robotic arm also reduces the load because the extension legs are no more needed. The carpet below the aerial manipulator provides visual features which ensure a good performance of the pose estimation method and reduce the pose estimation error.

Figure 10 depicts the block diagram for this research. The pose of the system when it is in fly mode is provided for the Visual SLAM technique. The movement of the robotic arm to fold and unfold produces a set of different disturbances. The objective of the attitude control is to reduce the displacement produced by this disturbance and any other disturbance induced by the outside conditions to maintain the aerial vehicle in the desired position. The proposed controller operates as external control, calculating the control signal u_d for the X- and Y-axes to displace the vehicle to the desired position; then, the u_d signals are sent to the internal control of Bebop-2. Finally, the pose estimation provided by the Visual SLAM closes the external control loop.

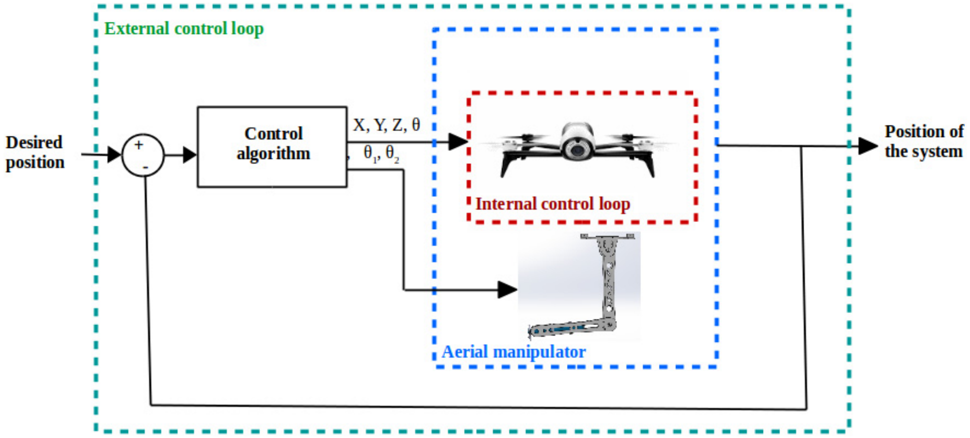

Fig. 10. Block diagram of the proposed system.

3.3. *Results*

Through several experimental tests, we studied the behavior of the system and tuned the parameters k_p and Γ of the control law expressed by Eqs. (11) and (10) to improve the performance of the complete system.

In the beginning, we choose the parameters according to our experience to study the behavior of the system and the control signal u_d. Figure 11 shows the response of the aerial manipulator at the beginning of the experiments.

Since the I&I technique is not a complex technique, after a few experiments, we were able to tune the value of the parameters and ensure the system reaches the desired position, and maintain the pose during the disturbances induced by the environment and the robotic arm. Figure 12 shows the first results of the experiments. The preliminary result shows that the proposed control strategy is able to lead the aerial manipulator to the desired point and maintain the position error close to zero. However, the control signal U switches between the limits of the range too quickly; this means that the aerial manipulator oscillates near to the desired point for a short time before stabilizing close to the reference. We upgraded the control strategy through the disturbance estimator to compensate for this behavior and increase the capabilities of the aerial manipulator to follow a desired trajectory. The disturbance estimator upgrade considers that the time derivative of the disturbance is not equal to zero; thus, it needs to be estimated. In this case, the disturbance estimator errors are

$$\delta_1 = \delta - \rho_1 - \Gamma_1 x$$
$$\delta_2 = \dot{\delta} - \rho_2 - \Gamma_2 x$$

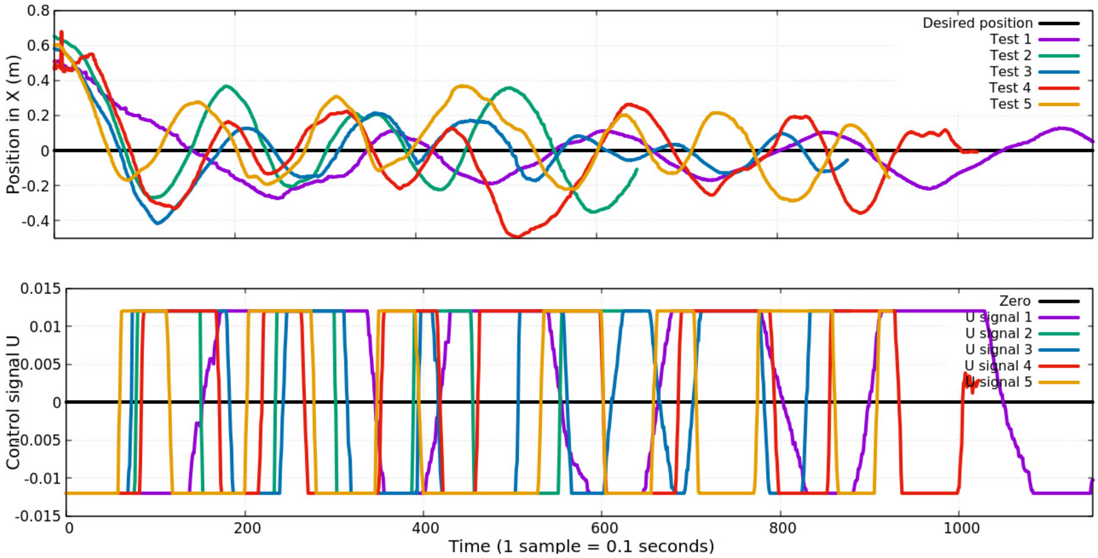

Fig. 11. Behavior of the aerial manipulator with the I&I control strategy. Initial experiments.

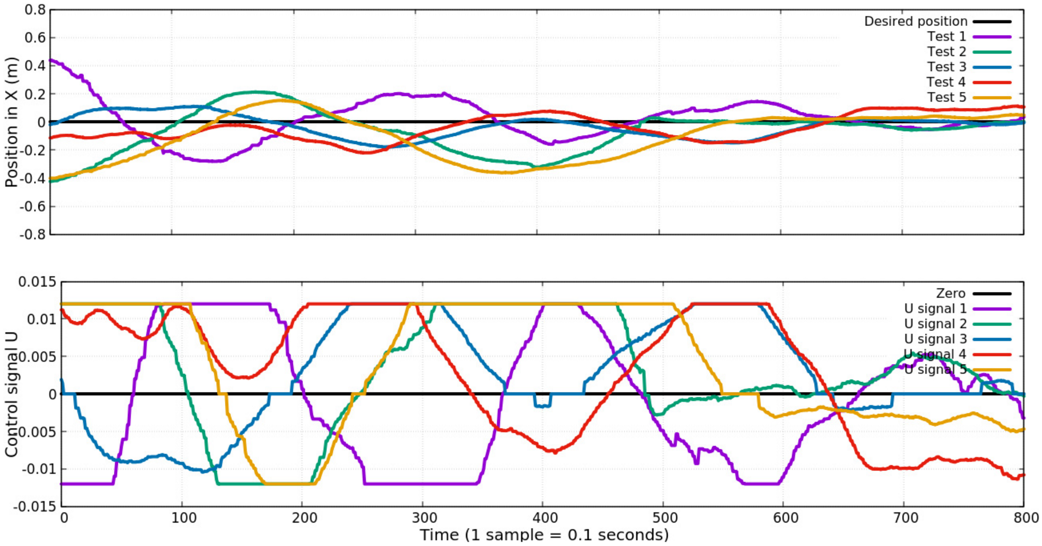

Fig. 12. Behavior of the aerial manipulator with the I&I control strategy. First results.

with δ_2 the time derivative disturbance estimation error, ρ_2 the estimator state and Γ_1, Γ_2 are positive gains. Defining

$$\begin{aligned} \dot{\rho}_1 &= \rho_2 + \Gamma_2 x - \Gamma_1(u_d + \rho_1 + \Gamma_1 x) \\ \dot{\rho}_2 &= -\Gamma_2(u_d + \rho_1 + \Gamma_1 x) \end{aligned} \tag{12}$$

it follows that

$$\begin{aligned} \dot{\delta}_1 &= -\Gamma_1 \delta_1 + \delta_2, \\ \dot{\delta}_2 &= -\Gamma_2 \delta_1 + \ddot{\delta}. \end{aligned}$$

Hence, if $\ddot{\delta}$ is equal zero, it is possible to select gains Γ_1 y Γ_2 such that δ_1 and δ_2 converge exponentially to zero. Since the control input can only compensate δ, u_d remains as defined in Eq. (11). Now, we have three gains, Γ_1, Γ_2, and K_p, to tune the control. After implementing the control expressed by Eq. (11) and the estimator in Eq. (12), we ran a few experiments, once again, to study the behavior of the improved control. The results of the second part of the experiments are shown in Fig. 13.

The results shown above were useful to select the appropriate values of the gains to improve the behavior of the aerial manipulator. The aerial manipulator follows the reference and maintains a stable flight when close to the desired position. The control signal U is not forced to the

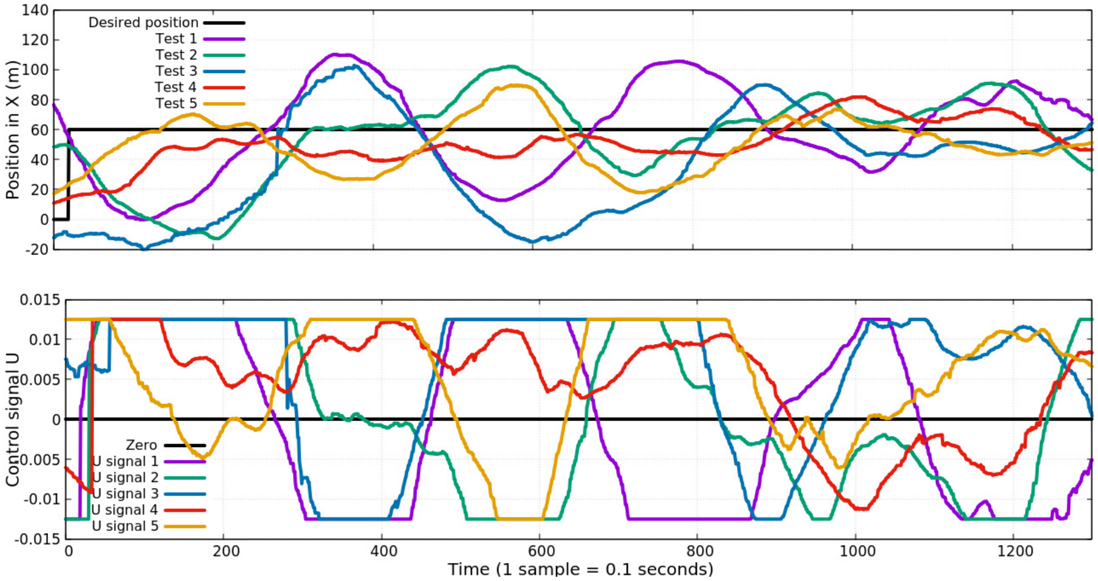

Fig. 13. Behavior of the aerial manipulator with the improved I&I control.

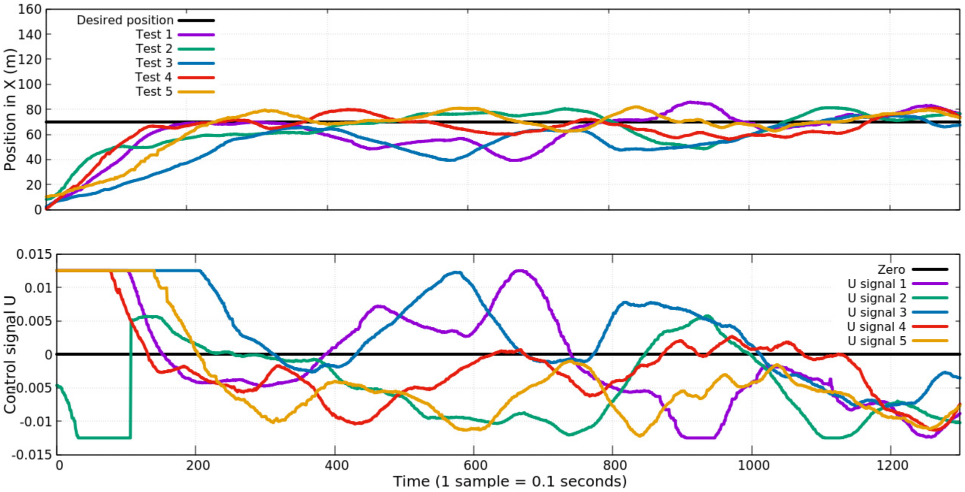

Fig. 14. Behavior of the aerial manipulator with the I&I control strategy. Second results.

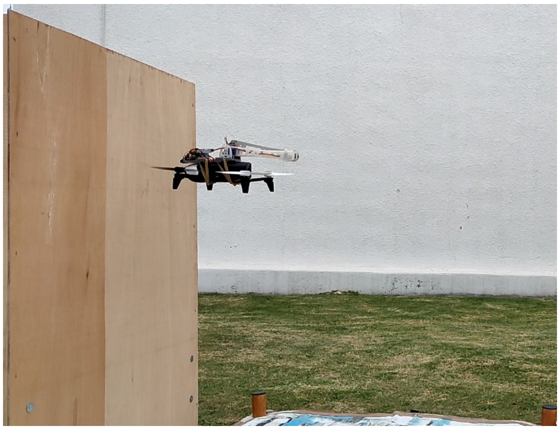

Fig. 15. Aerial manipulator near to a vertical surface. Video of experiments in the following URL: https://youtu.be/l_a4L8RlafE.

limits, and the oscillation was reduced according to the plots of Fig. 14. The results obtained in the second part of this work allow us to move forward in the aerial interaction experiments and to fly our aerial platform near a vertical surface to study the wall effect as a disturbance to the system.

Figure 15 shows the aerial manipulator flying close to a structure in an outdoor scenario. We sent the vehicle close enough to the structure (15 cm) to prove that our proposed control can maintain the aerial manipulator in a stable flight even with the disturbances induced by the vertical surface (wall-effect).

The parameters of the control strategy were tuned to obtain satisfactory results. Figure 16 shows the results of the final part of this work.

The final results proved that the proposed control strategy is able to send our aerial platform close to a

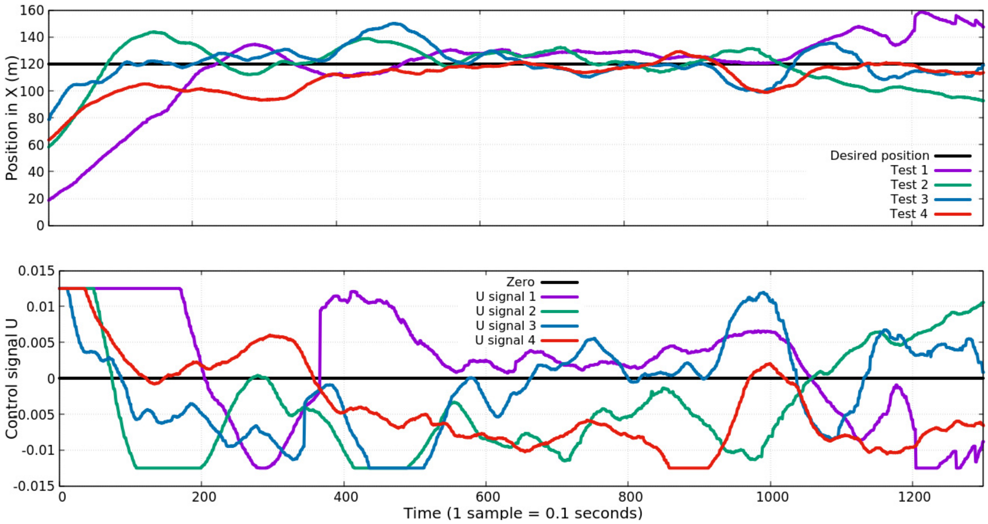

Fig. 16. Behavior of the aerial manipulator with the I&I control strategy. Final results.

structure and maintain a stable flight; this is essential to achieve a safety contact with the surface of the structure. In the final section, we discuss the conclusions and the future work of this research.

4. Conclusions and Future Work

In this work, a control strategy based on the I&I technique has been designed and implemented to control an aerial manipulator addressing issues related to the environment, the movement of the robotic arm, and the nearness of a vertical surface. The experimental results obtained for several tests are promising. A merit of the proposed algorithm is shown by the equations of the control law, which reduced the number of parameters of the controller, simplifying the experimental phase and allowing to obtain an efficient performance of the system. According to the results obtained in this work, we consider that the control could be tested in a scenario where the end-effector of the aerial manipulator makes full contact with a vertical surface and follow the desired trajectory without safety; this will be the subject of study in our future work.

References

[1] T. Bartelds, A. Capra, S. Hamaza, S. Stramigioli and M. Fumagalli, Compliant aerial manipulators: Toward a new generation of aerial robotic workers, *IEEE Robot. Autom. Lett.* **1**(1) (2016) 477–483.

[2] T. Wang, K. Umemoto, T. Endo and F. Matsuno, Dynamic hybrid position/force control for the quadrotor with a multi-degree-of-freedom manipulator, *Artif. Life Robot.* **24**(3) (2019) 378–389.

[3] A. L. Luna, I. C. Vega and J. Martinez-Carranza, Towards micro aerial manipulation using a computational compensation strategy, in *10th Int. Micro Air Vehicle Competition and Conf. (IMAV 2018)*, Vol. 11 (2018).

[4] F. Huber, K. Kondak, K. Krieger, D. Sommer, M. Schwarzbach, M. Laiacker, I. Kossyk, S. Parusel, S. Haddadin and A. Albu-Schiffer, First analysis and experiments in aerial manipulation using fully actuated redundant robot arm, in *2013 IEEE/RSJ Int. Conf. Intelligent Robots and Systems* (2013), pp. 3452–3457.

[5] C. Korpela, P. Brahmbhatt, M. Orsag and P. Oh, Towards the realization of mobile manipulating unmanned aerial vehicles (MM-UAV): Peg-in-hole insertion tasks, in *2013 IEEE Int. Conf. Technologies for Practical Robot Applications (TePRA)* (2013), pp. 1–6.

[6] H. Lee, S. Kim and H. J. Kim, Control of an aerial manipulator using on-line parameter estimator for an unknown payload, in *2015 IEEE Int. Conf. Automation Science and Engineering (CASE)* (2015), pp. 316–321.

[7] S. Di Lucia, G. D. Tipaldi and W. Burgard, Attitude stabilization control of an aerial manipulator using a quaternion-based backstepping approach, in *2015 Eur. Conf. Mobile Robots (ECMR)* (IEEE, 2015), pp. 1–6. DOI: 10.1109/ECMR.2015.7324191.

[8] A. Zulu and S. John, A review of control algorithms for autonomous quadrotors, *CoRR* (2016) abs/1602.02622.

[9] A. Dollar and P. E. I. Pounds, Hovering stability of helicopters with elastics constraints, *ASME Dynamic Systems and Control Conf.* (2010).

[10] M. Orsag, C. Korpela and P. Oh, Modeling and control of MM-UAV: Mobile manipulating unmanned aerial vehicle, *J. Intell. Robot. Syst.* **69**(1) (2013) 227–240.

[11] A. Astolfi and R. Ortega, Immersion and invariance: A new tool for stabilization and adaptive control of nonlinear systems, *IEEE Trans. Autom. Control* **48**(4) (2003) 590–606.

[12] J. Hu and H. Zhang, Immersion and invariance based command-filtered adaptive backstepping control of VTOL vehicles, *Automatica* **49**(7) (2013) 2160–2167.

[13] L. Wang, F. Forni, R. Ortega and H. Su, Immersion and invariance stabilization of nonlinear systems: A horizontal contraction approach, in *2015 54th IEEE Conf. Decision and Control (CDC)* (IEEE, 2015), pp. 3093–3097. DOI: 10.1109/cdc.2015.7402684.

[14] Y. Bouzid, H. Siguerdidjane and Y. Bestaoui, Real time autopilot based on immersion & invariance for autonomous aerial vehicle, *IFAC-PapersOnLine* **49**(17) (2016) 176–181, *20th IFAC Symp. Automatic Control in Aerospace (ACA) 2016*.

[15] G. Tagne, R. Talj and A. Charara, Immersion and invariance control for reference trajectory tracking of autonomous vehicles, in *16th Int. IEEE Conf. Intelligent Transportation Systems (ITSC 2013)* (IEEE, 2013), pp. 2322–2328. DOI: 10.1109/ITSC.2013.6728574.

[16] X. Li, H. Zhang, W. Fan, J. Zhao and C. Wang, Multivariable finite-time composite control strategy based on immersion and invariance for quadrotor under mismatched disturbances, *Aerosp. Sci. Technol.* **99**(2) (2020) 105763.

[17] L. O. Rojas-Perez and J. Martinez-Carranza, Metric monocular slam and colour segmentation for multiple obstacle avoidance in autonomous flight, in *2017 Workshop on Research, Education and Development of Unmanned Aerial Systems (RED-UAS)* (IEEE, 2017), pp. 234–239. DOI: 10.1109/RED-UAS.2017.8101672.

[18] J. J. Corona-Sánchez and H. Rodríguez-Cortés, Trajectory tracking control for a rotary wing vehicle powered by four rotors, *J. Intell. Robot. Syst.* **70**(1) (2013) 39–50.

[19] M. Fecko, *Differential Geometry and Lie Groups for Physicists* (Cambridge University Press, 2006).

[20] B. L. Stevens, F. L. Lewis and E. N. Johnson, *Aircraft Control and Simulation: Dynamics, Controls Design, and Autonomous Systems* (John Wiley & Sons, 2015).

[21] E. A. Morelli and V. Klein, *Aircraft System Identification: Theory and Practice*, Vol. 2 (Sunflyte Enterprises, Williamsburg, VA, 2016).

[22] Y. Huang and W. Xue, Active disturbance rejection control: Methodology and theoretical analysis, *ISA Trans.* **53**(4) (2014) 963–976, Disturbance Estimation and Mitigation.

[23] R. Seeber, M. Horn and L. Fridman, A novel method to estimate the reaching time of the super-twisting algorithm, *IEEE Trans. Autom. Control* **63**(12) (2018) 4301–4308.

[24] A. L. Luna, I. C. Vega and J. Martinez-Carranza, Gain-scheduling and pid control for an autonomous aerial vehicle with a robotic arm, in *2018 IEEE 2nd Colombian Conf. Robotics and Automation (CCRA)* (IEEE, 2018), pp. 1–6. DOI: 10.1109/CCRA.2018.8588145.

[25] A. L. Luna, J. Martinez-Carranza and I. C. Vega, Towards aerial interaction of MAVs in GPS-denied environments, in *2019 Workshop on Research, Education and Development of Unmanned Aerial Systems (RED UAS)* (IEEE, 2019), pp. 113–121. DOI: 10.1109/REDUAS47371.2019.8999686.

[26] H. Moon, J. Martinez-Carranza, T. Cieslewski, M. Faessler, D. Falanga, A. Simovic, D. Scaramuzza, S. Li, M. Ozo, C. De Wagter, G. de Croon, S. Hwang, S. Jung, H. Shim, H. Kim, M. Park, T.-C. Au and S. J. Kim, Challenges and implemented technologies used in autonomous drone racing, *Intell. Serv. Robot.* **12**(2) (2019) 137–148.

Aarón López Luna received his Master's degree in Engineering in Automatic Control from the Benemérita Universidad Autónoma de Puebla (BUAP) in 2016. He obtained Doctorate in Science from the Instituto Nacional de Astrofisica Optica y Electronica (INAOE) in 2020. His research interests include Robotics, Autonomous Systems, Automatic Control, and instrumentation. He is currently professor of Electronics and robotics courses since 2021.

Hugo Rodríguez-Cortés received B.S. degree in aeronautical engineering from the Instituto Politécnico Nacional (IPN), the M.Sc. degree in electrical engineering from the Centro de Investigación y de Estudios Avanzados del Instituto Politécnico Nacional (CINVESTAV-IPN), and the Ph.D. degree in automatic control and signal processing electrical from the Université de Paris XI, Gif-sur-Yvette, France. He held Postdoctoral appointments at the Control and Power Group, Imperial College of Science Technology and Medicine, London, UK, and the Department of Electrical and Computer Engineering, Northeastern University, Boston, MA, USA. He is currently a Researcher with the Mechatronics Section, Department of Electrical Engineering, CINVESTAV-IPN. His current research interests include control and state observation for unmanned aerial vehicles, energy-based control design, and real-time control. Dr. Rodríguez-Cortés serves as Associate Editor for the Journal of Intelligent and Robotic Systems.

Israel Cruz Vega received a degree in Control and Automation Engineering from the Instituto Politecnico Nacional. He obtained his Master's degree in Science and Doctor in Science degrees both in Automatic Control, from the Centro de Investigacion y de Estudios Avanzados of the Instituto Politecnico Nacional (CINVESTAV) in Mexico city.

After two years of postdoctoral research, he is now a CONACYT-research-fellow commissioned to the Instituto Nacional de Astrofisica, Optica y Electronica (INAOE) with the Electronics Department. His research interests are Automatic Control and Computational Intelligence applied to several engineering problems in bioengineering, automatic motor fault detection, control of autonomous aerial vehicles, prediction in chaotic systems, and Granular Computing and Deep Learning in time series prediction.

Jose Martinez-Carranza is Full-Time Principal Researcher B (equivalent to Associate Professor) in the Computer Science Department at the Instituto Nacional de Astrofisica Optica y Electronica (INAOE). He has published over 95 scientific papers in journals, international conferences, and book chapters. Currently, he leads the intelligent Unmanned Aerial Systems (iUAS) group at INAOE that has contributed to specialized topics in aerial robotics such as visual and auditory perception, aerial interaction, and autonomous navigation in GPS-denied environments using visual SLAM and spatial AI. In 2015, he was awarded the highly prestigious Newton Advanced Fellowship, and currently, he holds an Honorary Senior Research Fellowship in the Computer Science Department at the University of Bristol in the UK. His team has won international competitions such as 1st Place in the IEEE IROS 2017 Autonomous Drone Racing competition and first Place in the Regional Prize of the OpenCV AI Competition 2021, among others. He served as General Chair of the International Micro Air Vehicle conference, the IMAV 2021.